(19) Europäisches Patentamt
European Patent Office
Office européen des brevets

(11) EP 1 725 162 B1

(12) **EUROPEAN PATENT SPECIFICATION**

(45) Date of publication and mention of the grant of the patent:
19.04.2017 Bulletin 2017/16

(21) Application number: **05714607.8**

(22) Date of filing: **11.03.2005**

(51) Int Cl.:
A61B 3/14 *(2006.01)* ***G06T 3/00*** *(2006.01)*
A61B 3/12 *(2006.01)* ***A61B 5/00*** *(2006.01)*

(86) International application number:
PCT/CA2005/000367

(87) International publication number:
WO 2005/087088 (22.09.2005 Gazette 2005/38)

(54) **METHOD AND APPARATUS FOR DISPLAYING OCT CROSS SECTIONS**

VERFAHREN UND GERÄT ZUR ANZEIGE VON OCT-QUERSCHNITTEN

PROCEDE ET APPAREIL PERMETTANT D'AFFICHER DES SECTIONS TRANSVERSALES OCT

(84) Designated Contracting States:
AT BE BG CH CY CZ DE DK EE ES FI FR GB GR HU IE IS IT LI LT LU MC NL PL PT RO SE SI SK TR

(30) Priority: **11.03.2004 GB 0405416**

(43) Date of publication of application:
29.11.2006 Bulletin 2006/48

(73) Proprietor: **Optos PLC**
Fife, KY11 8GR (GB)

(72) Inventor: **PODOLEANU, Adrian**
Canterbury,
Kent CT2 7TU (GB)

(74) Representative: **Talbot-Ponsonby, Daniel Frederick**
Marks & Clerk LLP
Fletcher House
Heatley Road
The Oxford Science Park
Oxford OX4 4GE (GB)

(56) References cited:
WO-A1-2004/002298 **US-A- 5 384 608**
US-A1- 2003 103 212

- **OHMI M. ET AL: 'Optical reflection tomography along the goemetrical thickness.' SPIE PROC. PROGRESS IN BIOMEDICAL OPTICS AND IMAGING. vol. 4251, 2001, pages 76 - 80, XP010566157**
- **ZAWADSKI R.J. ET AL: 'Three-dimensional ophthalmic optical coherence tomography with a refraction correction algorithm.' SPIE PROC. vol. 5140, 2003, pages 20 - 27, XP002350080**
- **PODOLEANU A ET AL: "Correction of distortions in optical coherence tomography imaging of the eye", PHYSICS IN MEDICINE AND BIOLOGY IOP PUBLISHING UK, vol. 49, no. 7, 7 April 2004 (2004-04-07), pages 1277-1294, ISSN: 0031-9155**

EP 1 725 162 B1

Description

Field of the Invention

[0001] This invention relates to the field of Optical Coherence Tomography (OCT), and in particular to a method of displaying OCT sections of the retina of the eye.

Background of the Invention

[0002] Optical coherence tomography (OCT) is a powerful and sensitive tool for characterization of optical properties and imaging of superficial tissue, as described in the paper by D. Huang, E.A. Swanson, C. P. Lin, J. S. Schuman, W. G. Stinson, W. Chang, M. R. Hee, T. Flotte, K. Gregory, C. A. Puliafito and J. G. Fujimoto, 'Optical coherence tomography', published in Science 254, (1991) 1178-1181.

[0003] OCT can achieve micrometer depth resolution and allows accurate *in-vivo* measurement of thickness, area and volume in the tissue. In OCT, the depth dimension is explored by scanning the optical path difference (OPD) between the object path and reference path in an interferometer illuminated by a low coherence source. The maximum interference signal is obtained for OPD=0. In OCT, achievable depth resolution is given by the optical source line-width and not by the numerical aperture of the lens, as is the case in the confocal microscopy. For OPD values larger than the coherence length of the source used, the strength of the interference signal diminishes considerably. This explains the selection in depth of the OCT. Using a superluminescent diode (SLD) OCT depth resolution better than 15 μm is achievable. Employing a larger bandwidth source, 2 μm depth resolution becomes possible, as described in W. Drexler, U. Morgner, R. K. Ghanta, F. X. Kartner, J. S. Schuman, J. G. Fujimoto, "Ultrahigh-resolution ophthalmic optical coherence tomography", Nature Medicine, Vol. 7, No. 4, 502-507, 2001. OCT is an excellent method for high resolution imaging of superficial tissue, with penetration depths of up to 2-3 mm, depending on the scattering and absorption properties of the tissue.

[0004] A reflectivity depth profile called an A-scan is obtained by axial scanning. This means changing the OPD in the interferometer, for instance by moving the reference mirror in the reference arm.

[0005] B-scan images, which are analogous to ultrasound B-scan, are generated by collecting many A-scans for different and adjacent transverse positions, a method used in the paper by Huang mentioned above. The lines in the raster correspond to A-scans, i.e. the lines are oriented along the depth coordinate. The transversal scanner (operating along X or Y, or along the radius ρ or the polar angle θ in polar coordinates) advances at a slower pace to build a B-scan image.

[0006] Alternatively, a B-scan can be generated by using T-scans. In this case, the transversal scanner produces the fast lines in the image, as described in the papers by A. Gh. Podoleanu, G. M. Dobre, D. J. Webb, D. A. Jackson, "Coherence imaging by use of a Newton rings sampling function," Opt. Lett. 21, 1789-1791 (1996), by A. Gh. Podoleanu, G. M. Dobre, and D. A. Jackson, "En-face coherence imaging using galvanometer scanner modulation," Opt. Lett., 23, 147-149 (1998), and by A. Gh. Podoleanu, M. Seeger, G. M. Dobre, D. J. Webb, D. A. Jackson and F. Fitzke "Transversal and longitudinal images from the retina of the living eye using low coherence reflectometry," J. Biomed Optics, 3, 12-20 (1998). A T-scan can be produced by controlling either the transverse scanner along the X-coordinate, or along the Y-coordinate or along the radius ρ or the polar angle θ with the other transverse and axial scanners fixed. For instance, a T-scan based B-scan is obtained by driving the X-scanner to produce T-scans while the axial scanner advances slower in depth along the Z-coordinate.

[0007] A profile of reflectivity obtained while the depth scanning is fixed is called a T-scan. C-scans are made from many T-scans along either of X, Y, ρ or θ coordinates repeated for different values of the other transverse coordinate, Y, X, ρ or θ respectively in the transverse plane. The repetition of T-scans along the other transverse coordinate is performed at a slower rate than that of the T-scans, called the frame rate. In this way, a complete raster is generated. Different transversal slices are collected for different depths Z, either by advancing the optical path difference in the OCT in steps after each complete transverse (XY) or (ρ, θ) scan, or continuously at a much slower speed than the frame rate, as described in the paper by A.Gh.Podoleanu, J. A. Rogers, D. A. Jackson, S. Dunne, "Three dimensional OCT images from retina and skin", Opt. Express, Vol. 7, No. 9, 292-298, (2000), http://www.opticsexpress.org/abstract.cfm?URI=OPEX-7-9-292.

[0008] Typical errors in OCT imaging arise as a result of the specific way in which the image is constructed, i.e. from points of equal OPD, as described in the paper by M. Ohmi, K. Yoden and M. Haruna, "Optical reflection tomography along the geometrical thickness", Proc. SPIE, Vol. 4251, (2001), 76-80. Such errors are accumulated over the depth in the tissue and lead to deviations of zero OPD points from the position of the focus in confocal microscopy, as described in the paper by R. J. Zawadzki, C. Leisser, R. Leitgeb, M. Pircher, A. F. Fercher, 3D Ophthalmic OCT with a refraction correction algorithm, to be published in Proceed. SPIE, European Conf. Biomedical Optics, 22-25 June 2003, paper 5140-04. The error can exceed the depth resolution achievable with Kerr lens mode-locked lasers, and in some cases,

even the resolution achievable with superluminiscent diodes. The lateral errors also can amount to several pixels in the transverse section. These show that correction of images is paramount in order to obtain accurate, interpretable OCT images from the tissue. Diagnosis of glaucoma and macula degeneration relies on the instrument accuracy in determining the retina thickness. There is an increase demand for improving the resolution of the images collected.

[0009] Let us consider a curved surface separating two media of different indexes of refraction. The intersection of this surface with the plane y=0 is described by the contour Σ in Fig. 1. For any object point O(x,z), an image point I(h,v) is generated. We orient the axes of the object space and image space along parallel directions. The ray refracted in A, intersects the object point O. The distance in the medium is AO.

[0010] Let us consider the medium homogenous of index of refraction n. The frame grabber puts the image point I in the plane (h,v) at a distance from the image point A, equal to the distance AO multiplied by the index of refraction, n. We define two errors, an axial and a lateral error. For instance, in the case of an A-scan, the user expects to collect points from along the line AI in Fig. 1, but in fact the OCT system acquires data along the line AO and places them along the line AI.

[0011] When performing a B-scan, if the normal to the surface Σ deviates from the plane of Fig. 1, the B-scan will contain points from the volume outside the plane of Fig. 1.

[0012] For C-scanning, the user expects to collect an image from a plane II, perpendicular to the axis OZ. However, due to the curvature of the surface Σ, the coherence gate selects points from inside the object situated on a curved surface, S.

[0013] Superposing the origins of the object space and image space in point C, the lateral error E^l and the axial error E^a are defined as:

$$E^l = |x - h| \tag{1a}$$

$$E^a = |z - v| \tag{1b}$$

[0014] The axial error includes the elongation of the image in depth due to the index of refraction, n, of the medium or different media intersected by the ray up to the point O. Optical coherence tomography (OCT) images are collected from the retina with different scanning procedures. The present invention relates to B-scan images, i.e. images containing the optic axis and oriented in depth. First OCT images of the retina have been produced as B- scans, constructed from many A-scans at different transverse positions. An A-scan is a profile of reflectivity in depth.

[0015] Development of en-face OCT leads to scanning the retina transversally or angularly.

[0016] By putting together many T-scans for different depth positions, again a B scan image of the tissue is obtained.

[0017] However, all images so far have been presented as rectangular, i.e. as made of line oriented laterally and axially at 90 degrees. In reality, the eye ball is round.

[0018] US patent application no. 2003/0103212 describes a number of techniques for correcting for various image distortions in OCT scanning including distortions resulting from radial scanning.

Summary of the Invention

[0019] The present invention relates to a method wherein B-scan images or deep layers within the B-scan images are conveniently bent to represent more closely the shape of the tissue at the back of the eye.

[0020] In accordance with the present invention there is provided a method of creating OCT cross sectional images of the retinal pigment epithelium of an eye under examination, the method comprising: determining the length of the eye; scanning the retinal pigment epithelium (RPE) with an OCT light beam in a fan configuration from a convergence point in the pupil to create an array of image points defined by Cartesian coordinates (h,v) in an image space; transforming said array of image points in said image space to an array of points defined by polar coordinates (r,α) from said convergence point in an object space taking into account the length of the eye and the refractive index within the retina, n; wherein the polar coordinates and the Cartesian coordinates are related by:

$$h=2H\alpha/\alpha_M;$$

$$v=Vz/z_M;$$

and

$$r=r_0+z/n;$$

where 2H is a number of image points along the h axis, V is a number of image points along the v axis, α_M is a maximum optical ray deflection angle, z is the position of an axial scanner, and z_M is the maximum axial range of the axial scanner; said image points being further transformed taking into account the foveal pit height, $z_f - z_R$, and the index of refraction of the vitreous, n_v, and the average index of refraction of the fovea, n_r and wherein the point on the RPE in the center of the fovea is lowered by $\delta = (n_r - n_v)(z_f - z_R)$ and all points either side are lowered by proportionally less value as the lateral distance up to an axis perpendicular on the fovea through the foveal pit; displaying said array of points in the object space on a display device to provide an OCT cross sectional image of the retina

[0021] Disclosed herein is a method of a method of creating OCT cross sectional images of the retinal pigment epithelium of an eye under examination, comprising: determining the length of the eye; scanning the retinal pigment epithelium with an OCT light beam in a fan configuration from a convergence point in the pupil to create an array of image points defined by a Cartesian coordinate system in an image space; transforming said array of image points in said image space to an array of points defined by polar coordinates from said convergence point in an object space taking into account the length of the eye and the refractive index within the eye; and displaying said array of points in the object space on a display device to provide an OCT cross sectional image of the retina, said image points being transformed taking into account the foveal pit height, H, and the index of refraction of the vitreous, nv, and the average index of refraction of the fovea, nr and wherein the point on the RPE in the center of the fovea is lowered by and all points either side are lowered by proportionally less value as the lateral distance up to an axis perpendicular on the fovea through the foveal pit.

[0022] The invention can compensate for distortions introduced, for example, by fan scanning, different refractive indices within the object, or depressions for the object surface. The invention is particularly applicable to OCT images of the eye, especially the human eye, in which case the layers of the retina and vitreous have different refractive indices and the fovial depression introduces further distortion.

Brief Description of the Drawings

[0023] The invention will now be described in more detail, by way of example only, with reference to the accompanying drawings, in which:

Figure 1 shows x,z: object space; h,v: image space; Surface Σ: separates media of different refractive indices; points along the line AO are placed in the image along the line AI, corresponding to a single vertical line in the generated OCT image; S: distorted surface of OPD = constant.

Figure 2 illustrates the acquisition of an OCT image by fan scanning the object ray.

Fig. 3 shows the distorted image of a microscope slide when scanned with a fan of rays.

Figures 4a and 4b illustrate the bending images of the retina upwards to compensate for fan scanning distortion. The image in the square centred on the fovea of the normal subject is used in the processing of the RPE layer as described below.

Figure 5 shows the evaluation of the refraction angle at the interface between the vitreous and the retina.

Figure 6 is an exaggerated representation of the distortion of the RPE contour.

Detailed Description of the Preferred Embodiments

[0024] OCT can be implemented, for example, with apparatus described in detail in US Patent no. 5,975,697. The described processing can be carried out with a personal computer, for example, including a Pentium™ microprocessor.

[0025] The invention will be described with reference to the eye, although it will be understood that it could be applied to other objects having similar structure.

[0026] Consider the case of angular OCT scanning of the eye, where the fan of rays converges in a point C, as illustrated in Fig. 2. This is the scanning pattern when imaging the retina. A collimated beam is scanned angularly through

the anterior part of the eye, where refractive elements focus it on the retina. The top part of Fig. 2 shows the fan of rays scanning the retina The bottom part represents the image acquired by the OCT for arc circles with the center in C. Polar coordinates, r, a and a corresponding Cartesian system with axes x and z are defined for the object space with the center located in the eye pupil, C. For the image space, a simple Cartesian coordinate system (h,v) is used. The relation between a point in the object space O(r, a) and the corresponding point in the image space I(h,v) needs to be understood.

[0027] The frame grabber of the OCT system places the B-scan image in the plane (h,v), where:

$$\begin{aligned} h &= k_h \alpha, \\ v &= k_v z \end{aligned} \qquad (2a,b)$$

z is the axial movement of the reference mirror from the initial position. k_h and k_v are scanning scaling factors for the transverse and axial scanner respectively. k_h is given by the number of sample pixels along the horizontal axis, 2H, divided by the maximum optical ray deflection angle, α_M.k_v is given by the number of vertical sample pixels in the image along the vertical axis V, divided by the maximum axial range, z_M covered by the axial scanner in the reference arm of the OCT interferometer.

$$\begin{aligned} k_h &= \frac{2H}{\alpha_M} \\ k_v &= \frac{V}{z_M} \end{aligned} \qquad (3a,b)$$

[0028] The axial scanner varies the reference path to select points within the retina, situated at a certain radial distance between r_0 and $r_0+\Delta r$. If the scanner moves by z, then the coherence gated spatial window advances from the initial position r_0 to:

$$r = r_0 + \frac{z}{n} \qquad (3c)$$

where n is the average index of refraction of the retina, considered a constant, 1.38 everywhere in the eye for brevity.

[0029] Placing the reference for OPD = 0 in the top centre of the image o and also making the object space and the image space coincide in this point, lateral and vertical errors produced by the fan scanning can be computed as:

$$\begin{aligned} E^l &= (r_0 + \frac{z}{n}) \sin \alpha \\ E^a &= (r_0 + \frac{z}{n}) \cos \alpha - r_0 \end{aligned} \qquad (4a,b)$$

[0030] E^1 measures how much the image point I moves laterally relative to the corresponding object point O, while E^a signifies how much the image point I moves axially from the corresponding object point O. For a null α angle, the errors are zero.

[0031] To better understand the distortions in the fan scanning case, let us consider a simple rectangular object, such as a microscope slide glass in Fig. 3 left. During scanning, for a certain fixed OPD in the OCT apparatus, the coherence gate selects those points from the object situated on an arc of circle with the centre in C and radius matching the reference arm length. Under these circumstances, the anterior surface Σ_1 appears in the image (Fig. 3 right) as a curved line, S_1. The same is true for the other surface, Σ_2 whose image is described by S_2. The example in Fig. 3 shows that an horizontal shape of the object surface is represented as a downward curved surface in the image space. This means that the images collected by fan scanning type have to be corrected by curving them up.

[0032] For points on the anterior surface, Σ_1, the polar coordinates in the object space are:

$$O(\frac{r_0}{\cos\alpha}, \text{artc tan}\frac{x}{r_0}) \quad (5)$$

[0033] In Cartesian coordinates h and v, the points of the anterior surface Σ_1 will be located in the B-scan image at points:

$$I(h,v) = (k_u \, artc\tan\frac{x}{r_0}, \frac{k_v r_0}{\cos\alpha} - k_v r_0) \quad (6)$$

[0034] These equations show that the higher the angle α either side of the axis oz, the larger the vertical distortion of the image. A horizontal line in the object is represented as a downwardly curved line in the image space. Similarly, the second surface, Σ_2, given by points

$$O(d + \frac{r_0}{\cos\alpha}, \text{artc tan}\frac{x}{r_0}) \quad (7)$$

will be transferred to a curved line:

$$I(h,v) = I(k_u \, artc\tan\frac{x}{r_0}, k_v d + \frac{k_v r_0}{\cos\alpha} - k_v r_0) \quad (8)$$

in the image plane, (h,v). The corrected image is shown in the right hand side of Fig. 4.

[0035] We inversed equations of type 6 and 8 written for each point in the image to correct T-scan based B-scan images obtained from the retina. The correction exercise is exemplifies on two images shown in Figs. 4a and 4b, that of a normal eye and of a case of neuroretinitis with optic disc edema and peripapillary serous detachment of the neurosensory retina. To correct the images, we used an average eye length of 24 mm for a normal subject, the experimental angular span of 35^0 and an average index of refraction n = 1.38 as presented in literature, as for example in E. Chen, Eye Laboratory, Ophthalmic Res., 25, (1993), 65-68 and in M.Hammer, D.Schweitzer, E.Thamm, A.Kolb, "Optical Properties of ocular fundus tissues determined by optical coherence tomography", Opt. Commun., 186, 149-153, 2000.

[0036] It is important to associate the pathology location to the eye curvature, which is correct in the images bent upwards. For the numerical values used, the axial error is 1.2 mm and lateral error 0.44 mm. Although it is possible to estimate the eye length, for more accurate results, OCT should be first used to evaluate the eye length value, and input to the evaluations above.

Correction of the RPE and CC layer orientation

[0037] A second aspect of the disclosure is the correction of orientation of layers just below the foveal pit. These layers are important for correct diagnosis of eye diseases.

[0038] A B-scan OCT image of the fovea obtained with T-scanning is shown in Fig. 4a top left. Let us select a small lateral size image around the fovea as that inside the square superposed on the image. The lateral size is small and for simplicity, we choose to ignore here the distortion due to fan scanning presented previously. Due to the cumulated effect of (i) different indexes of refraction of the vitreous and of the retina and (ii) of the foveal depression, the image of the deep layers in the retina is distorted. For instance, an histological image of the fovea shows that the retinal pigment epithelium (RPE) is a straight oriented layer. However, due to the effects mentioned above, the RPE layer is slightly curved upwards. It is the scope of the present invention to evaluate quantitatively the distortion of the shape of the RPE layer and its upward deviation from a straight line. Let us consider the index of refraction of the vitreous, n_v= 1.336, and of the retina up to the RPE, n_r= 1.35.

[0039] The OCT image sampled by the square in Fig. 4a top left could be transferred to a calibrated chart containing orthogonal co-ordinate systems (ox to the right, oz downwards) or digitally sampled. The contours of the foveal pit can then be approximated by analytical curves:

$$z = f(x) \quad (19)$$

[0040] In the same system of coordinates, the equation of the middle of the RPE can be approximated by:

$$z_p = cons\tan t \qquad (20)$$

[0041] The ray coming from the vitreous is incident on the retina in A_j. The equation of the refracted line A_jB_j is written for a point $A_j(x_j,z_j)$ on the inner limiting membrane (ILM) described by equation (19), as:

$$x - x_j = m(z - z_j) \qquad (21)$$

[0042] The slope is:

$$m = \tan[\frac{\pi}{2} \pm (\theta_j - \theta)] \qquad (22)$$

[0043] The incidence angle, θ_j is

$$6_j = \pi \pm \gamma \qquad (23)$$

where γ is given by:

$$\tan\gamma = \frac{dz}{dx} \qquad (24)$$

evaluated in each point A_j.

[0044] We can calculate the coordinate of each point B_j on the RPE where the line described by the equation (21) intersects the RPE described by equation (20), and obtain the points of coordinates (x_p,z_p). If the origin of the optical path length in the vitreous is at a coordinate $z = z_0$ (a reference line is shown in Fig. 5), then the optical path length can be evaluated as:

$$v = n_v(z_j - z_0) + n_r\sqrt{(x_j - x_p)^2 + (z_j - z_p)^2} \qquad (25)$$

[0045] This determines the shape of the RPE layer in Fig. 6. The deviation of the RPE layer from straight line is small and therefore, to illustrate the distortion, the bottom part below the broken line in Fig. 6 is represented at a vertical scale multiplied 10 times.

[0046] In points such as B_f and B_p, where the ray comes along the normal to the retina (like points in the center, A_f or outside the fovea region, A_R respectively), the x coordinates are the same and the optical path length is:

$$v_f = n_v(z_f - z_0) + n_r(z_p - z_f) \qquad (26a)$$

or

$$v_R = n_v(z_R - z_0) + n_r(z_p - z_R) \qquad (26b)$$

[0047] The elevation of the RPE in the center of the image can be simply calculated by subtracting equation (26a) from (26b) which gives:

$$\delta = (n_r - n_v)(z_f - z_R) \qquad (27)$$

[0048] Considering a normal average foveal pit value H = (z_f - z_R) = 150 μm and the values for the indexes of refraction of the vitreous, n_v=1.336, and of the retina up to the RPE, n_r= 1.35, δ = 2.1 μm. Such a deviation is hard to be noticed in Fig. 5 due to the resolution, 12 μm of an SLD based OCT system. However, this deviation is comparable to the depth resolution achievable in high resolution OCT imaging of the fovea.

Claims

1. A method of creating OCT cross sectional images of the retinal pigment epithelium of an eye under examination, comprising:

   determining the length of the eye;
   scanning the retinal pigment epithelium, RPE, with an OCT light beam in a fan configuration from a convergence point in the pupil to create an array of image points defined by Cartesian coordinates (h,v) in an image space;
   transforming said array of image points in said image space to an array of points defined by polar coordinates (r,α) from said convergence point in an object space taking into account the length of the eye and the refractive index within the retina, n;
   wherein the polar coordinates and the Cartesian coordinates are related by:

   $$h=2H\alpha/\alpha_M;$$

   $$v=Vz/z_M;$$

   and

   $$r=r_0+z/n;$$

   where 2H is a number of image points along the h axis, V is a number of image points along the v axis, α_M is a maximum optical ray deflection angle, z is the position of an axial scanner, and z_M is the maximum axial range of the axial scanner;
   said image points being further transformed taking into account the foveal pit height, z_f - z_R, and the index of refraction of the vitreous, n_v, and the average index of refraction of the fovea, n_r and wherein the point on the RPE in the center of the fovea is lowered by δ = (n_r - n_v)(z_f - z_R) and all points either side are lowered by proportionally less value as the lateral distance up to an axis perpendicular on the fovea through the foveal pit;
   displaying said array of points in the object space on a display device to provide an OCT cross sectional image of the retina.

2. A method as claimed in claim 1, wherein the length of the eye is measured with an OCT apparatus.

3. A method as claimed in claim 1, wherein the length of the eye is estimated.

4. A method as claimed in claim 1 wherein the foveal pit height H is evaluated using OCT and the indexes of refraction are n_v = 1.336, and of the retina up to the RPE, n_r = 1.35.

Patentansprüche

1. Verfahren zum Erzeugen von OCT-Querschnittsbildern des Netzhautpigmentepithels eines untersuchten Auges, umfassend:

   Bestimmen der Länge des Auges;

Abrastern des Netzhautpigmentepithels, RPE, mit einem OCT-Lichtstrahl in einer Fächerkonfiguration von einem Konvergenzpunkt in der Pupille, um eine Anordnung von Bildpunkten zu erzeugen, die durch kartesische Koordinaten (h, v) in einem Bildraum definiert ist;
Transformieren der Anordnung von Bildpunkten in dem Bildraum in eine Anordnung von Bildpunkten, die durch Polarkoordinaten (r, α) von dem Konvergenzpunkt in einem Objektraum definiert ist, wobei die Länge des Auges und der Brechungsindex innerhalb der Netzhaut, n, berücksichtigt werden;
worin die Polarkoordinaten und die kartesischen Koordinaten verknüpft sind durch:

$$h = 2H\alpha/\alpha_M;$$

$$v = Vz/z_M;$$

und

$$r = r_0 + z/n;$$

wobei 2H eine Anzahl von Bildpunkten entlang der h-Achse ist, V eine Anzahl von Bildpunkten entlang der v-Achse ist, α_M ein maximaler optischer Strahlablenkungswinkel ist, z die Position eines Axialscanners ist und z_M die maximale axiale Reichweite des Axialscanners ist;
wobei die Bildpunkte ferner unter Berücksichtigung der Höhe der Fovea-Grube, $z_f - z_R$, und des Brechungsindex der Glaskörperflüssigkeit, n_v, und des mittleren Brechungsindex der Fovea, n_r, transformiert werden und worin der Punkt auf dem RPE im Zentrum der Fovea um $\partial = (n_r - n_v)(z_f - z_R)$ abgesenkt wird und alle Punkte auf beiden Seiten um proportional kleinere Werte als der seitliche Abstand zu einer senkrecht auf der Fovea stehenden Achse durch die Fovea-Grube abgesenkt werden;
Anzeigen der Anordnung von Punkten im Objektraum auf einer Anzeigevorrichtung, um ein OCT-Querschnittsbild der Netzhaut bereitzustellen.

2. Verfahren nach Anspruch 1, worin die Länge des Auges mit einem OCT-Gerät gemessen wird.

3. Verfahren nach Anspruch 1, worin die Länge des Auges geschätzt wird.

4. Verfahren nach Anspruch 1, worin die Höhe der Fovea-Grube H unter Verwendung von OCT bewertet wird und die Brechungsindizes $n_v = 1{,}336$ und für die Retina bis zum RPE $n_r = 1{,}35$ betragen.

Revendications

1. Procédé de création d'images en coupe transversale, par TCO tomographie par cohérence optique, de l'épithélium pigmentaire rétinien d'un oeil en cour d'examen, comprenant les étapes consistant à :

déterminer la longueur de l'oeil ;
balayer l'épithélium pigmentaire rétinien, EPR, avec un faisceau lumineux TCO selon une configuration d'éventail à partir d'un point de convergence situé au niveau de la pupille afin de créer un réseau des points d'image, définis par des coordonnées cartésiennes (h, v), au sein d'un espace-image ;
transformer ledit réseau de points d'image au sein dudit espace-image en un réseau de points, définis par des coordonnés polaires (r, α) à partir dudit point de convergence, au sein d'un espace-objet en prenant en compte la longueur de l'oeil et l'indice de réfraction de la rétine, n ;
dans lequel les coordonnées polaires et les coordonnés cartésiennes sont liées par les relations :

$$h = 2H\alpha/\alpha_M ;$$

$$v = Vz/z_M ;$$

et

$$r = r_0 + z/n ;$$

dans lequel 2H est un nombre de points d'image le long de l'axe h, V est un nombre de points d'image le long de l'axe v, α_M est un angle maximal de déviation de rayon optique, z est la position d'un dispositif de balayage axial, et z_M est l'étendue axiale maximale du dispositif de balayage axial ;
lesdits points d'image étant en outre transformés en prenant en compte la hauteur de la dépression fovéale, $z_f - z_R$, et l'indice de réfraction du vitré, n_v, et l'indice moyen de réfraction de la fovéa, n_r, et dans lequel le point situé sur l'EPR au centre de la fovéa est diminué d'une valeur $\delta = (n_r - n_v)(z_f - z_R)$ et tous les points situés de chaque côté sont diminués d'une valeur proportionnellement inférieure à la distance latérale les séparant d'un axe perpendiculaire situé sur la fovéa et passant par la dépression fovéale ;
afficher ledit réseau de points au sein de l'espace-objet sur un dispositif d'affichage afin de fournir une image en coupe transversale TCO de la rétine.

2. Procédé selon la revendication 1, dans lequel la longueur de l'oeil est mesurée avec un appareil TCO.

3. Procédé selon la revendication 1, dans lequel la longueur de l'oeil est estimée.

4. Procédé selon la revendication 1, dans lequel la hauteur H de la dépression fovéale est évaluée en utilisant un dispositif TCO et les indices de réfraction sont $n_v = 1,336$, et, les indices de la rétine jusqu'à l'EPR, $n_r = 1,35$.

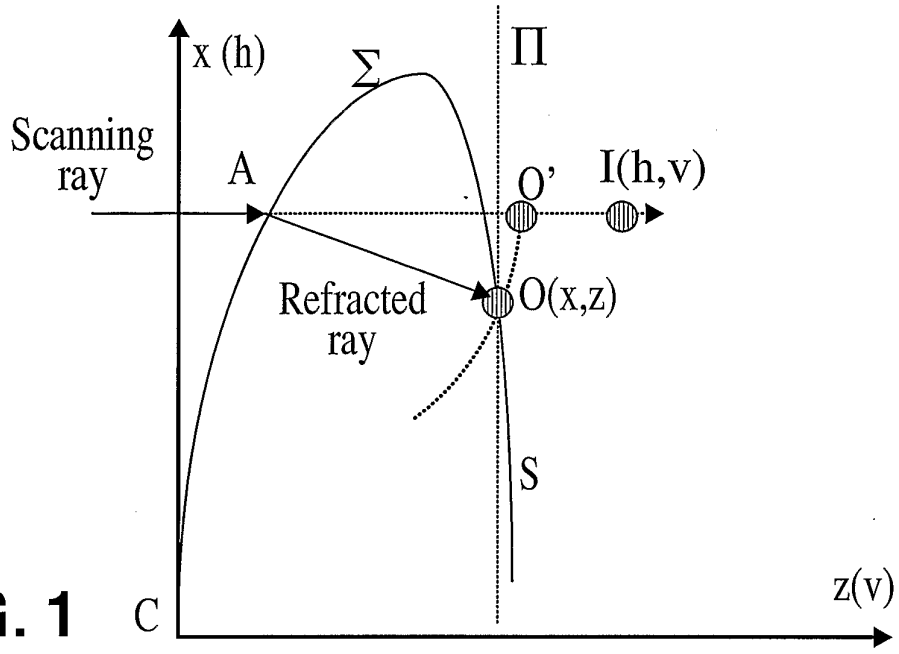
x (h)
Σ
Π
Scanning ray
A
O'
I(h,v)
Refracted ray
O(x,z)
S
C
z(v)

FIG. 1

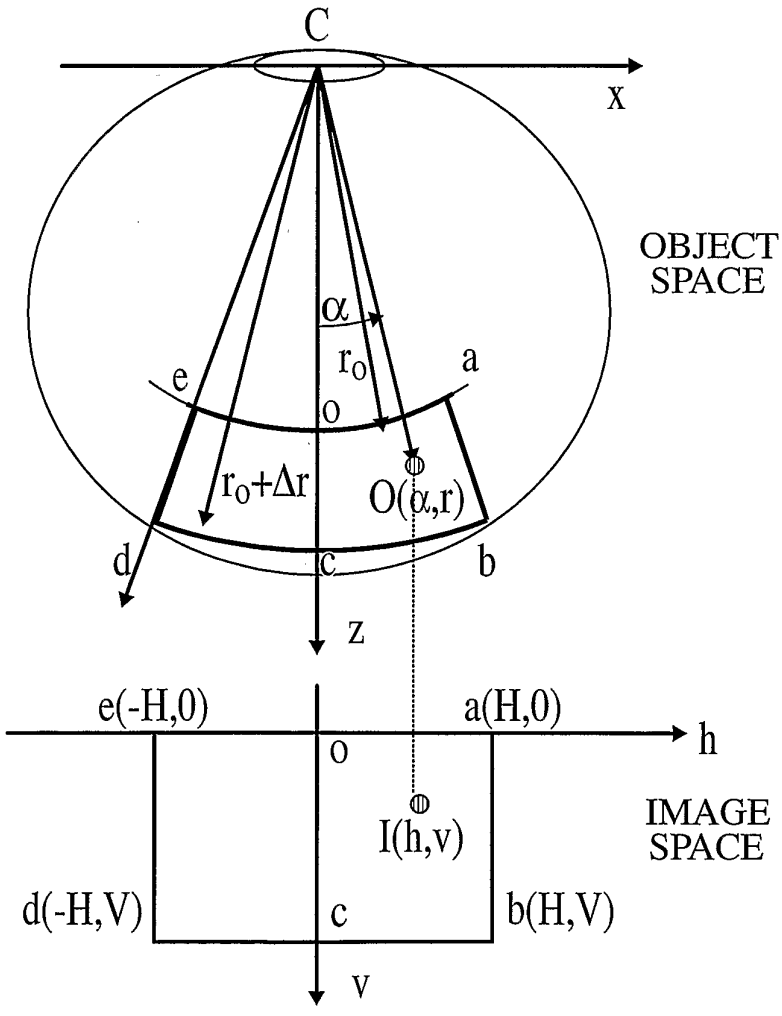
C
x
OBJECT SPACE
α
r0
a
e
o
r0+Δr
O(α,r)
d
c
b
z
e(-H,0)
a(H,0)
h
o
I(h,v)
IMAGE SPACE
d(-H,V)
c
b(H,V)
v

FIG. 2

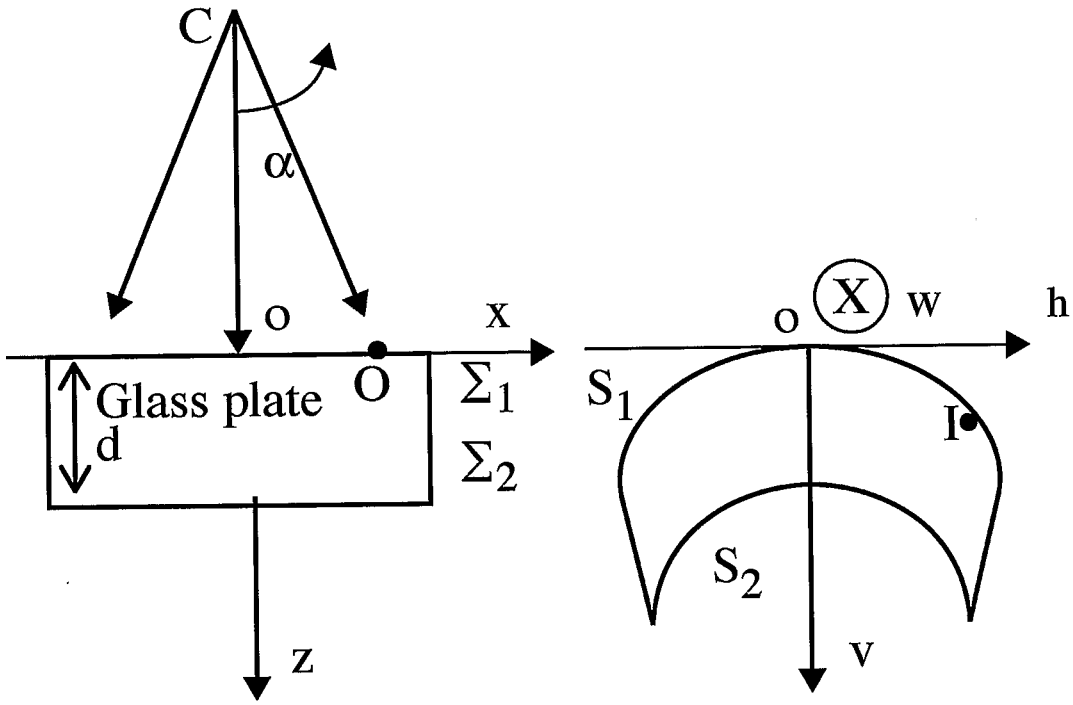

FIG. 3

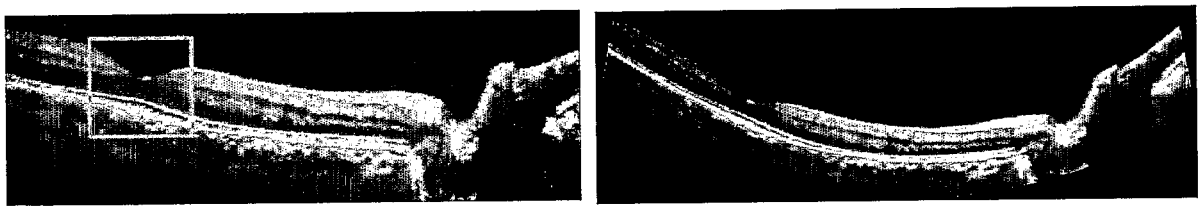

Normal fovea

FIG. 4a

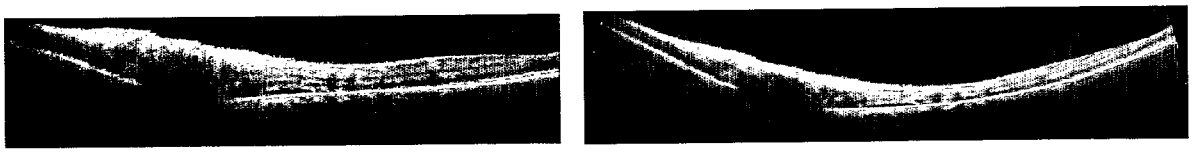

Neuronitis with optic disc edema and peripapillary serous detachment

FIG. 4b

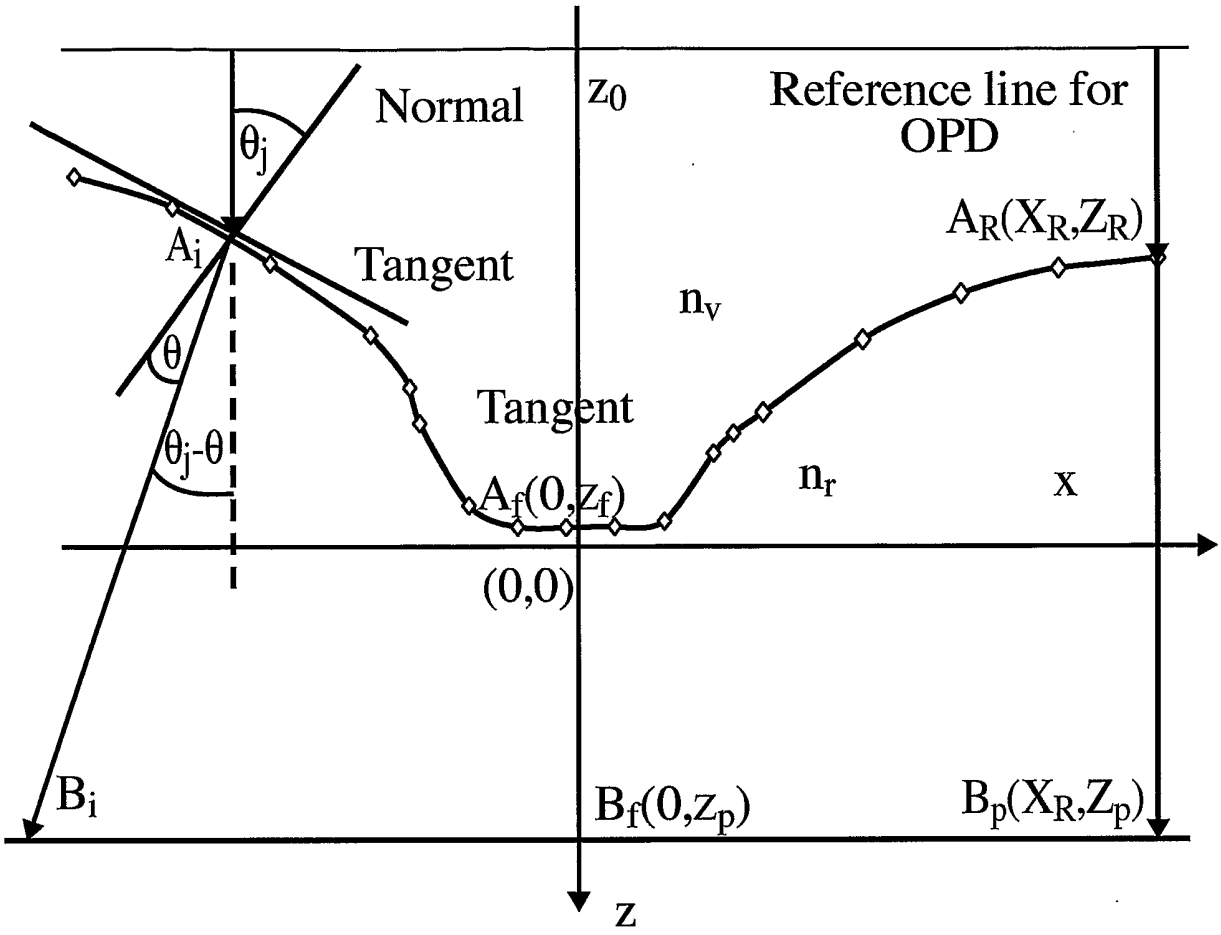

FIG. 5

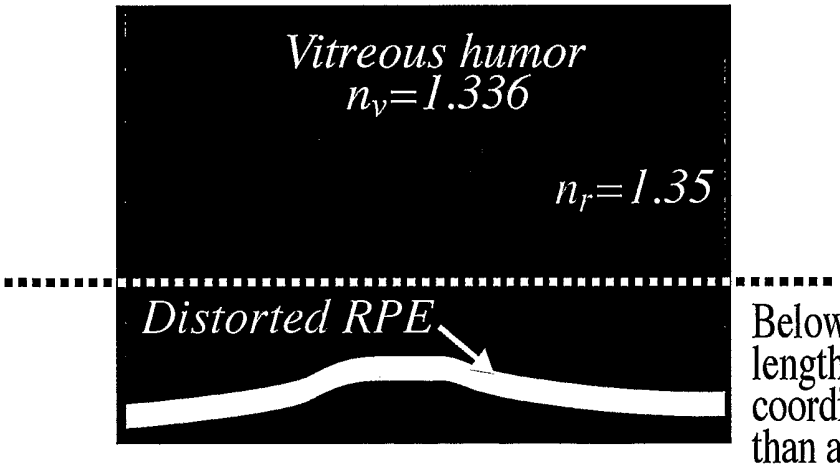

Below the broken line, the unit length along the vertical coordinate is 10 times smaller than above the line.

FIG. 6

REFERENCES CITED IN THE DESCRIPTION

This list of references cited by the applicant is for the reader's convenience only. It does not form part of the European patent document. Even though great care has been taken in compiling the references, errors or omissions cannot be excluded and the EPO disclaims all liability in this regard.

Patent documents cited in the description

- US 20030103212 A **[0018]**
- US 5975697 A **[0024]**

Non-patent literature cited in the description

- **D. HUANG ; E.A. SWANSON ; C. P. LIN ; J. S. SCHUMAN ; W. G. STINSON ; W. CHANG ; M. R. HEE ; T. FLOTTE ; K. GREGORY ; C. A. PULIAFITO.** Optical coherence tomography. *Science,* 1991, vol. 254, 1178-1181 **[0002]**
- **W. DREXLER ; U. MORGNER ; R. K. GHANTA ; F. X. KARTNER ; J. S. SCHUMAN ; J. G. FUJIMOTO.** Ultrahigh-resolution ophthalmic optical coherence tomography. *Nature Medicine,* 2001, vol. 7 (4), 502-507 **[0003]**
- **A. GH. PODOLEANU ; G. M. DOBRE ; D. J. WEBB ; D. A. JACKSON.** Coherence imaging by use of a Newton rings sampling function. *Opt. Lett.,* 1996, vol. 21, 1789-1791 **[0006]**
- **A. GH. PODOLEANU ; G. M. DOBRE ; D. A. JACKSON.** En-face coherence imaging using galvanometer scanner modulation. *Opt. Lett.,* 1998, vol. 23, 147-149 **[0006]**
- **A. GH. PODOLEANU ; M. SEEGER ; G. M. DOBRE ; D. J. WEBB ; D. A. JACKSON ; F. FITZKE.** Transversal and longitudinal images from the retina of the living eye using low coherence reflectometry. *J. Biomed Optics,* 1998, vol. 3, 12-20 **[0006]**
- **A.GH.PODOLEANU ; J. A. ROGERS ; D. A. JACKSON ; S. DUNNE.** Three dimensional OCT images from retina and skin. *Opt. Express,* 2000, vol. 7 (9), 292-298, http://www.opticsexpress.org/abstract.cfm?URI=OPEX-7-9-292 **[0007]**
- **M. OHMI ; K. YODEN ; M. HARUNA.** Optical reflection tomography along the geometrical thickness. *Proc. SPIE,* 2001, vol. 4251, 76-80 **[0008]**
- **R. J. ZAWADZKI ; C. LEISSER ; R. LEITGEB ; M. PIRCHER ; A. F. FERCHER.** 3D Ophthalmic OCT with a refraction correction algorithm. *Proceed. SPIE, European Conf. Biomedical Optics,* 22 June 2003, 5140-04 **[0008]**
- **E. CHEN.** *Eye Laboratory, Ophthalmic Res.,* 1993, vol. 25, 65-68 **[0035]**
- **M.HAMMER ; D.SCHWEITZER ; E.THAMM ; A.KOLB.** Optical Properties of ocular fundus tissues determined by optical coherence tomography. *Opt. Commun.,* 2000, vol. 186, 149-153 **[0035]**

专利名称(译)	用于显示八字形横截面的方法和设备		
公开(公告)号	EP1725162B1	公开(公告)日	2017-04-19
申请号	EP2005714607	申请日	2005-03-11
[标]申请(专利权)人(译)	OTI眼科TECH		
申请(专利权)人(译)	OTI-OPHTHALMIC技术有限公司		
当前申请(专利权)人(译)	OPTOS PLC		
[标]发明人	PODOLEANU ADRIAN		
发明人	PODOLEANU, ADRIAN		
IPC分类号	A61B3/14 G06T3/00 A61B3/12 A61B5/00 G01B9/02		
CPC分类号	A61B3/102 G01B9/02083 G01B9/02091		
优先权	2004005416 2004-03-11 GB		
其他公开文献	EP1725162A4 EP1725162A1		
外部链接	Espacenet		

摘要(译)

通过创建一系列图像点并将每个图像点放置到校正图像中来显示弯曲物体的一部分的OCT截面图像，使得图像内的散射点的位置与或至少更接近于它们在弯曲物体内的真实空间分布。